

Seven-dimensional microcanonical treatment of hydrogen dissociation dynamics on Cu(111): Clarifying the essential role of surface phonons

H. L. Abbott and I. Harrison^{a)}

Department of Chemistry, University of Virginia, Charlottesville, Virginia 22904-4319

(Received 24 March 2006; accepted 2 May 2006; published online 13 July 2006)

A simple picture of the hydrogen dissociation/associative desorption dynamics on Cu(111) emerges from a two-parameter, full dimensionality microcanonical unimolecular rate theory (MURT) model of the gas-surface reactivity. Vibrational frequencies for the reactive transition state were taken from density functional theory calculations of a six-dimensional potential energy surface [Hammer *et al.*, *Phys. Rev. Lett.* **73**, 1400 (1994)]. The two remaining parameters required by the MURT were fixed by simulation of experiments. These parameters are the dissociation threshold energy, $E_0 = 79$ kJ/mol, and the number of surface oscillators involved in the localized H₂/Cu(111) collision complex, $s=1$. The two-parameter MURT quantitatively predicts much of the varied behavior observed for the H₂ and D₂/Cu(111) reactive systems, including the temperature-dependent associative desorption angular distributions, mean translational energies of the associatively desorbing hydrogen as a function of rovibrational eigenstate, etc. The divergence of the statistical theory's predictions from experimental results at low rotational quantum numbers, $J \leq 5$, suggests that either (i) rotational steering is important to the dissociation dynamics at low J , an effect that washes out at high J , or (ii) molecular rotation is approximately a spectator degree of freedom to the dissociation dynamics for these low J states, the states that dominate the thermal reactivity. Surface vibrations are predicted to provide $\sim 30\%$ of the energy required to surmount the activation barrier to H₂ dissociation under thermal equilibrium conditions. The MURT with $s=1$ is used to analytically confirm the experimental finding that $\partial "E_a(T_s)"/\partial E_t = -1$ for eigenstate-resolved dissociative sticking at translational energies $E_t < E_0 - E_v - E_r$. Explicit treatment of the surface motion (i.e., surface not frozen at $T_s=0$ K) is a relatively novel aspect of the MURT theoretical approach.

© 2006 American Institute of Physics. [DOI: 10.1063/1.2208362]

I. INTRODUCTION

Hydrogen dissociative chemisorption on Cu(111) is often considered to be the quintessential model system for gas-surface reactivity.¹⁻³ Calculation of the reactive H₂/Cu(111) potential energy surface remains a formidable challenge for electronic structure theory even though it involves the simplest molecule dissociating on a closed shell, first row, transition metal surface.⁴ The wealth of detailed experimental data on the H₂/Cu(111) reactive system^{3,5-18} provides unsurpassed opportunities for testing theoretical models of gas-surface reactivity. With the recent interest in developing alternative energy sources (e.g., H₂ fuel cells), achieving a molecular-level understanding of the surface reactivity of the H-H bond is an increasingly pressing scientific concern. There is currently no consensus amongst experimentalists and theorists on the threshold energy for H₂ dissociation on Cu(111). The roles of dynamical steering and surface atom motion have been largely neglected or decoupled by theory, even in the most recent, high level, quantum dynamical calculations.^{4,19-27} In this paper, we employ a full dimensionality microcanonical unimolecular rate theory²⁸⁻³⁰ (MURT) to model a large number of experimental results and arrive at a simple unified description of the dissociative

chemisorption/associative desorption dynamics. The two required MURT parameters fixed by experiments are the dissociation threshold energy, $E_0 = 79$ kJ/mol, and the number of surface oscillators involved in the localized H₂/Cu(111) collision complex, $s=1$.

Early experiments by Rendulic and co-workers measured the initial dissociative sticking coefficient S of hydrogen on Cu(111) as a function of translational energy using seeded supersonic molecular beams.^{16,17} Further beam experiments by Auerbach and co-workers showed that both vibrational energy and normal translational energy (i.e., $E_n = E_t \cos^2 \vartheta$) promote the dissociative sticking of H₂ and D₂ on Cu(111).^{8-10,13} The kinetic isotope effect in these experiments, approximately 1.3 for H₂ versus D₂, is sufficiently small that tunneling is not considered to play a major role in the reactive dynamics. Thermal associative desorption experiments are able to explore the roles of molecular vibrational, rotational, and translational (E_v, E_r, E_t) energies on the dissociative sticking via the principle of detailed balance.^{8,31} Detailed balance asserts that the thermal associatively desorbing hydrogen flux should exactly balance the flux of hydrogen that would successfully dissociatively stick under thermal equilibrium conditions, even at quantum-state-resolved levels of detail. In this way, studies of associative desorption can provide detailed information about the reverse process, dissociative sticking. The angular distribution

^{a)}Fax: (434) 924-3710. Electronic mail: harrison@virginia.edu

of associatively desorbing hydrogen is peaked around the surface normal as $\sim \cos^n \vartheta$ with $10 \leq n \leq 19$ dependent on surface temperature T_s . The ~ 60 kJ/mol mean translational energy for D_2 desorbing from Cu(111) at $T_s=1000$ K provides evidence for exit channel repulsion over a substantial barrier to dissociative chemisorption.¹⁸ Auerbach and co-workers measured the translational energy distributions of desorbing hydrogen as a function of rovibrational state (ν, J) .^{8,10,12} They pointed out that a distribution of barriers to reaction is sampled during dissociative chemisorption experiments due to uncontrolled averaging over molecular orientation, vibrational phase, and impact position across the surface unit cell.³² Progress was made by asserting that different rovibrational states experience different effective dissociation barriers that can be quantified, to some degree, by fitting rovibrationally resolved translational energy distributions of recombinatively desorbing hydrogen to an empirically derived error-function (erf) based sticking form.^{8,10,33} At low J , the $\langle E_t(\nu, J) \rangle$ of hydrogen that successfully sticks increases slightly with J up until $J \sim 5$, consistent with the effective barrier to reaction increasing with rotational energy and rotational energy hindering sticking. The decrease in $\langle E_t(\nu, J) \rangle$ at higher J is consistent with a lowering of the effective barrier to reaction with J and so further rotational energy enhances sticking. The preference for helicoptering rotational alignment (i.e., with angular momentum vector \mathbf{J} along the surface normal such that the molecular bond is broadside to the surface) of the successfully sticking molecules was found to decrease with increasing translational energy and increase with increasing rotational energy.^{6,7} By monitoring the associative desorption of H_2 and D_2 from Cu(111),⁵ Murphy and Hodgson determined surface temperature dependent, molecular eigenstate-resolved relative sticking coefficients and calculated “effective activation energies” $E_a(T_s) = -k_B \partial \ln S / \partial (T_s^{-1})$. The effective activation energies for the molecular eigenstate-resolved sticking decreased linearly with the molecular translational energy [i.e., $\partial E_a(T_s) / \partial E_t \approx -1$]. In sum, this diverse set of detailed experimental observations provides a challenging set of criteria by which to critically assess models of gas-surface reactivity.

Gross *et al.*²⁶ used time-independent quantum scattering theory applied to two-dimensional (2D) and five-dimensional (5D) potential energy surfaces (PESs) derived from generalized gradient approximation (GGA)-density functional theory (DFT) to calculate sticking coefficients that were compared to values derived from H_2 dissociative chemisorption and associative desorption experiments.¹⁴ The theoretical $S(E_t)$ sticking coefficient underestimated the experimental sticking by a ΔE_t shift of ~ 20 kJ/mol which led the theorists to suggest a threshold energy for reaction of $E_0 \approx 48$ kJ/mol instead of the $E_0=70$ kJ/mol value of their 5D GGA-DFT PES. Quantum scattering theory²⁶ was also used to calculate the $\langle E_t(\vartheta) \rangle$ and angular flux distribution of desorbing hydrogen for comparison to experimental values measured by Comsa and David.¹⁸ Reasonable agreement was obtained for the mean translational energies, but the calculated angular distribution was considerably sharper than the experimental $\cos^n \vartheta$ fit [i.e., $n_{\text{theory}}=25$ for $H_2/\text{Cu}(111)$ versus $n_{\text{expt}}=8$ for $D_2/\text{Cu}(100)$ at $T_s=1000$ K (Ref. 18)]. Re-

cently, on a more fully converged GGA-DFT-derived PES, Sakong and Gross found the threshold energy for reaction to be $E_0=48.5$ kJ/mol,²⁰ in good accord with the expectation of the earlier scattering study.

A benchmark GGA-DFT-derived six dimensional (6D) PES calculated by Hammer *et al.* also has a threshold energy of $E_0 \approx 48$ kJ/mol.²⁵ The transition state has H_2 parallel to the surface and centered over a bridge site. Transition state vibrational frequencies from this PES are used in our MURT modeling below. Recent 6D wave packet calculations, which include all molecular degrees of freedom but not the surface degrees of freedom, have examined the behavior of eigenstate-resolved H_2 and D_2 scattering from Cu(111) using several PESs with E_0 varying from 52 to 69 kJ/mol.^{4,21} Dai and Light have explored the role of steric effects on the dissociation of hydrogen and have determined that “helicopter” rotational motion (i.e., angular momentum vector \mathbf{J} along the surface normal) promotes reaction more than “cartwheel” rotational motion (i.e., \mathbf{J} in the surface plane).^{22,23}

Holloway and co-workers have theoretically studied the effects of surface temperature on the reactivity of hydrogen on Cu.^{19,27} They simulated recombinative desorption experiments similar to those of Murphy and Hodgson⁵ using high dimensionality wave packet calculations on a four-dimensional (4D) PES coupled to a single Einstein surface oscillator.¹⁹ The 4D PES had a reaction threshold energy of $E_0 \sim 67.5$ kJ/mol for broadside approach of H_2 on Cu(111). The wave packet calculations gave Arrhenius dissociative sticking behavior for $D_2(\nu=1, J=0)$ with a slope of $\partial E_a(T_s) / \partial E_t = -0.86$ over the range of 29 kJ/mol $\leq E_t \leq 35$ kJ/mol, while at higher E_t the slope diminished rapidly towards zero. Experimental values of $\partial E_a(T_s) / \partial E_t$ were -0.92 and -0.97 for H_2 and D_2 , respectively, in the ground vibrational state over the range of 5 kJ/mol $\leq E_t \leq 60$ kJ/mol.⁵ A semianalytical quantum mechanical model and a semiclassical surface mass model^{34,35} that couples the surface to molecular reactive and energy transfer processes were compared by Wang *et al.*¹⁹ and it was argued that Arrhenius behavior should be seen with $\partial E_a(T_s) / \partial E_t$ approaching -1 for all gas-surface processes characterized by a high threshold energy and multiphonon excitation.

Dynamical steering has been theoretically explored for H_2 on Cu(111) using a variety of quantum and classical dynamics techniques.^{36,37} The idea is that slowly translating and rotating molecules may be most easily steered by long range forces into the most favorable orientation for reaction (e.g., by application of torque for sufficient time) and thereby experience enhanced sticking. Conversely, molecules translating and rotating quickly (i.e., in high J states, particularly when executing the relatively unfavorable cartwheel motion) cannot be easily steered into the preferred broadside geometry as they approach the surface and, therefore, have lower sticking coefficients. Reduced dimensionality wave packet calculations including only the cartwheel component of rotational motion were able to reproduce the qualitative trends of the experimental $\langle E_t(\nu, J) \rangle$ behavior but this consistency was lost when azimuthal rotation was included in full three-dimensional (3D) rotor simulations.³⁷ Since quantum and classical dynamics simulations give similar dissociative

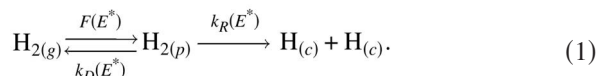
sticking results as a function of energy, quantum effects, such as tunneling, do not seem to play an important role in the reactivity of hydrogen on copper.³⁶

If dynamical steering is strong then the initial alignment of the incident molecules should be irrelevant to their sticking and so by detailed balance associatively desorbing molecules should exhibit relatively little rotational alignment. Experimentally, this seems to be the case for low $J \leq 5$.⁷ For $J > 5$ there is an increasing preference for helicoptering rotational alignment with increasing J and the alignment decreases with increasing translational energy.⁶ Consequently, with increasing J , dynamical steering diminishes and the steric importance of broadside attack of hydrogen on Cu(111) becomes increasingly evident. However, as the translational energy increases at fixed high J , and the total energy available to surmount the reaction barrier increases, the molecules need not take the very minimum energy pathway to dissociate (i.e., broadside approach) and the importance of sterics diminishes as evidenced by diminishing rotational alignment as the translational energy increases.

A three-parameter MURT local hot spot model of gas-surface reactivity has sufficed to quantitatively treat the dissociative chemisorption dynamics of polyatomic molecules, such as CH₄,^{38–40} SiH₄,⁴¹ and C₂H₆,⁴² on several different surfaces. In this paper, we employ transition state vibrational frequencies from the 6D GGA-DFT PES of Nørskov and co-workers for the H₂/Cu(111) reactive system^{24,25} to formulate a MURT model with only two adjustable parameters. Of particular interest is to assess the applicability and limitations of the statistical MURT model for the H₂/Cu(111) reactive system, presumably the gas-surface system where the MURT approximation of ensemble-averaged microcanonical randomization of the initial energy in the gas-surface collision complexes is likely to be most tenuous and where quantum effects are most likely to be observable. Perhaps surprisingly, the two-parameter MURT model quantitatively captures much of the observed hydrogen dissociative sticking behavior. The full dimensionality MURT model is also helpful as a statistical baseline against which dynamical effects, such as steering or rotational energy conservation, can be identified when they occur.^{29,40,42} The surface plays an essential role in the gas-surface reaction dynamics and roughly 30% of the energy required to surmount the activation barrier for H₂ dissociation on Cu(111) derives from the surface under thermal equilibrium conditions.

II. PHYSISORBED COMPLEX-MICROCANONICAL UNIMOLECULAR RATE THEORY (PC-MURT)

The MURT local hot spot model^{28–30} is illustrated schematically in Fig. 1 and assumes that the activated H₂ dissociative chemisorption kinetics can be described microcanonically as



The zero of energy E^* ($=E_t + E_v + E_r + E_s$) occurs at 0 K with infinite separation between the surface and H₂. Hydrogen incident on the surface forms a transient gas-surface collision

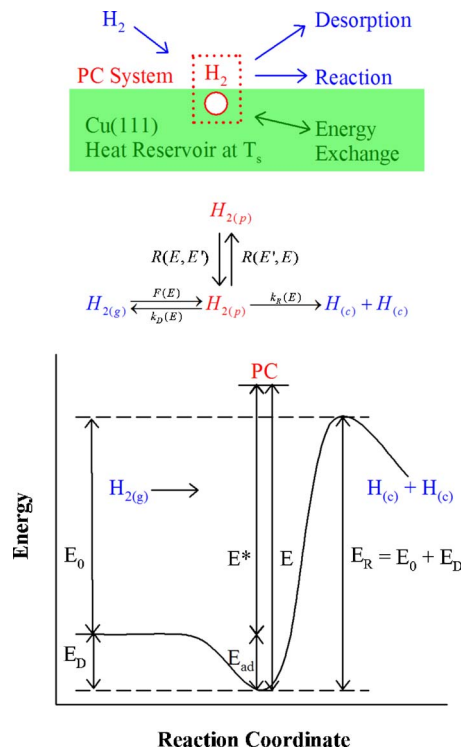


FIG. 1. Schematic depiction of the kinetics and energetics for the activated dissociation of H₂ on Cu(111). Surface coordination numbers have been suppressed in the kinetic equation and the zero point energies are implicitly included in the 2D potential energy curve along the reaction coordinate.

complex consisting of the molecule and a few adjacent surface atoms represented as s surface oscillators. This local hot spot is an energetic, transient intermediate species, which is not in thermal equilibrium with the remainder of the substrate. Energy in this transiently formed physisorbed complex [PC or H₂(p) in Eq. (1)] is assumed to be microcanonically randomized in an ensemble averaged sense either through the collision process itself or through rapid intramolecular vibrational energy redistribution (IVR). A PC formed with total energy E^* subsequently either competitively desorbs or reacts with Rice-Ramsperger-Kassel-Marcus (RRKM) rate constants $k_D(E^*)$ and $k_R(E^*)$. Ultrafast PC desorption rates at reactive energies for the H₂/Cu(111) system lead to negligible energy exchange with the surrounding substrate. The physisorbed complex-microcanonical unimolecular rate theory (PC-MURT) neglects energy transfer between the PC and surrounding surface heat bath [e.g., by setting the energy transfer rates $R(E', E)$ to 0 in Fig. 1 kinetics], and thereby treats the PC as an adiabatic system.

Applying the steady state approximation to the H₂(p) coverage of Eq. (1) yields an expression for the initial dissociative sticking coefficient that is measured experimentally,

$$S = \int_0^\infty S(E^*) f(E^*) dE^*, \quad (2)$$

where

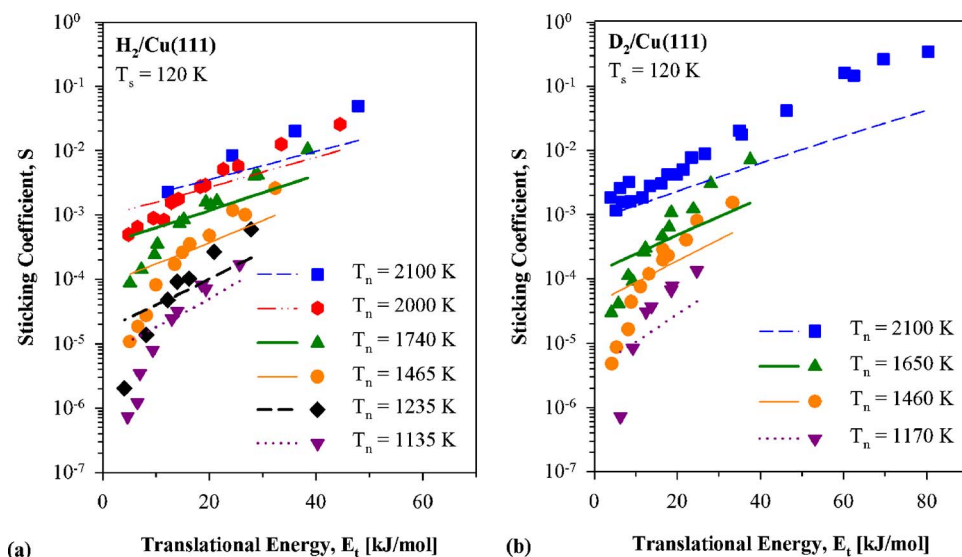


FIG. 2. Absolute dissociative sticking coefficients for thermally populated molecular beams of (a) H_2 (Ref. 8) and (b) D_2 (Ref. 10) at specified nozzle temperatures (points) are compared to PC-MURT simulations (lines). The sharp slope of the experimental sticking as a function of energy suggests a high entropic factor and a loose reactive transition state. The ARD between the molecular beam sticking and the PC-MURT is 206%.

$$S(E^*) = \frac{W_R^\ddagger(E^* - E_0)}{W_R^\ddagger(E^* - E_0) + W_D^\ddagger(E^*)} \quad (3)$$

is the microcanonical sticking coefficient, W_i^\ddagger is the sum of states for transition state process i , E_0 is the apparent threshold energy for dissociation, and

$$f(E^*) = \int_0^{E^*} f_t(E_t) \int_0^{E^* - E_t} f_v(E_v) \times \int_0^{E^* - E_t - E_v} f_r(E_r) f_s(E^* - E_t - E_v - E_r) dE_r dE_v dE_t \quad (4)$$

is the flux distribution for creating a physisorbed complex at E^* . The $f(E^*)$ results from the convolution over the individual energy distribution functions for each degree of freedom: the flux weighted translational energy, vibrational energy, and rotational energy of the incident hydrogen, along with the surface energy distribution for s surface oscillators vibrating at the mean Cu phonon frequency, $\nu_s = \frac{3}{4} k_b \theta_{\text{Debye}} / h$, of 175 cm^{-1} . Centrifugal and anharmonic corrections were used in determining the hydrogen rotational and vibrational en-

ergy levels. The vibrational energy levels were calculated as $E_v(\nu) = \nu\omega_e - \nu(\nu+1)\omega_e x_e$ and the rotational energy levels were calculated as $E_r(J) = hc[B_e J(J+1) - D_e J^2(J+1)^2]$.⁴³ Nuclear spin statistics were incorporated in the PC-MURT under the assumption that spin flips did not occur during the PC residence time on the surface (e.g., para- H_2 incident on the surface could only desorb as para- H_2 or dissociate). Consequently, dissociative sticking from the ortho and para molecules was calculated separately and then averaged in the experimentally observed abundance ratios of 3:1 for H_2 and 2:1 for D_2 .⁴⁴

Molecular beam studies of H_2 dissociative chemisorption on Cu(111) find that the initial sticking coefficient scales with the translational energy directed along the surface normal, $^{13}E_n = E_t \cos^2 \vartheta$. Consequently, we discount parallel molecular translational energy as a spectator or inactive form of energy over the course of the reactive gas-surface collisions and apply the dynamical constraint that only normal translation will contribute to E_t in the equations above (i.e., set $E_t = E_n$ alone). In accordance with experimental observations, we further assume that the molecular beam nozzle

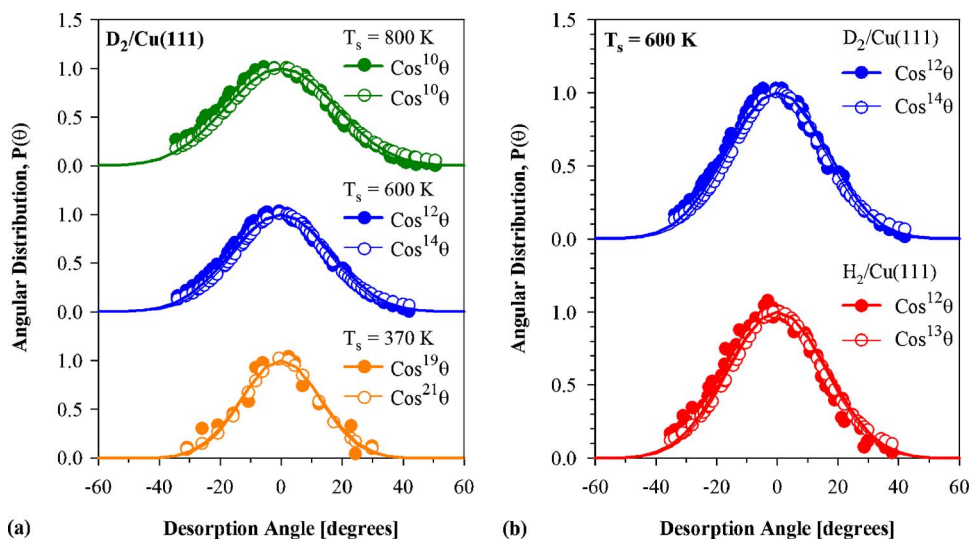


FIG. 3. Experimental (solid points and bold lines) (Refs. 8 and 10) and PC-MURT (open points and thin lines) angular distributions and $\cos^n \theta$ fits for H_2 and D_2 recombinative desorption from Cu(111) at various surface temperatures are displayed. 5D quantum calculations predict a sharply peaked angular distribution of $\cos^{25} \theta$ for H_2 on Cu(111) at $T_s = 1000$ K (Ref. 26). The ARD=23% for these angular distributions.

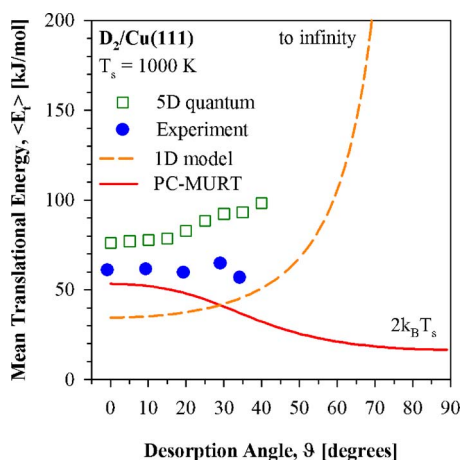


FIG. 4. Experimental mean translational energies for recombinative desorption as a function of angle (solid points) (Ref. 18) are compared to 5D quantum calculations (open points) (Ref. 26), van Willigen model calculations (dashed line) (Ref. 46), and PC-MURT predictions (solid line). The ARD between the experiment and (i) the PC-MURT is 33%, (ii) the 5D quantum calculations is 39%, and (iii) the van Willigen model is 59%.

temperature T_n , sets the vibrational and rotational temperatures of the beam molecules as $T_v = T_n$ and $T_r = 0.9T_n$, respectively.⁸

In past examples where the PC-MURT was applied to dissociative chemisorption of polyatomic molecules, full characterization of the transition state was not directly available from electronic structure theory calculations and so three adjustable parameters were used to characterize the transition state: s , the number of surface oscillators vibrating at the mean substrate phonon frequency that are able to freely exchange energy within the PC; E_0 , the threshold energy for reaction; and ν_D , a mean vibrational frequency characteristic of the three frustrated rotations and the vibration of the molecule along the direction of the surface normal at the transition state. All other vibrational frequencies of the transition state were assumed to be the same as in the gas-phase molecule far from the surface.

For the hydrogen/Cu(111) system, we chose to take the

vibrational frequencies for the transition state from the 6D GGA-DFT PES of Nørskov and co-workers and allow only s and E_0 to be free parameters in our MURT modeling. The transition state for desorption is taken to occur when hydrogen is freely rotating and vibrating in the gas phase far from the surface. The reactive transition state is characterized by s surface oscillators vibrating at the mean Cu phonon frequency of 175 cm^{-1} , the cartwheel and helicopter frustrated rotations, and the vibration of H_2 along the surface normal. The H–H vibrational mode is sacrificed as the reaction coordinate. From the 6D PES, the vibrational frequencies of the frustrated rotations (cartwheel and helicopter) and perpendicular vibration within the physisorption potential well are 1050 , 805 , and 405 cm^{-1} , respectively.^{24,25} The two adjustable parameters, E_0 and s , of the resulting PC-MURT are fixed by minimizing the average relative discrepancy (ARD) between theoretical predictions and experimental values, e.g., for sticking, according to

$$\text{ARD} = \left\langle \frac{|S_{\text{theor}} - S_{\text{expt}}|}{\min(S_{\text{theor}}, S_{\text{expt}})} \right\rangle. \quad (5)$$

A strength of the MURT analysis is that once the transition state characteristics have been defined by fits to experimental data or (in principle) by electronic structure theory calculations, the dependence of an experimental sticking coefficient on any dynamical variable (T_s , E_t , E_v , etc.) can be predicted on the basis of Eq. (2) by averaging the microcanonical sticking coefficient over the probability for creating a physisorbed complex at E^* under the specific experimental conditions of interest. Worth explicitly noting is that the PC-MURT provides a *statistical* description of the dissociative chemisorption dynamics as can be seen from the microcanonical sticking coefficient of Eq. (3) which is simply the ratio of the available exit channels through the reactive transition state to the total number of exit channels available through either the reactive or desorptive transition states.

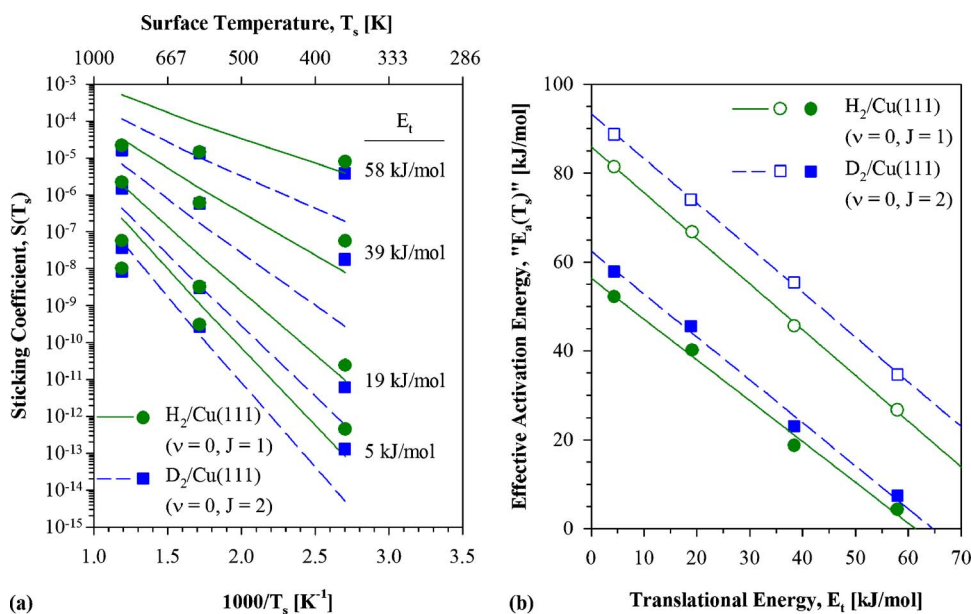


FIG. 5. (a) Surface temperature dependent, relative dissociative sticking coefficients obtained from recombinative desorption experiments (solid points) (Ref. 5) have been scaled to give optimal agreement with PC-MURT predictions (lines) based on absolute molecular beam sticking coefficients (Refs. 8 and 10). Despite the scaling, the ARD=1106%. (b) Effective activation energies derived from Arrhenius plots of the sticking coefficients shown in (a) are plotted for experiment (solid points) (Ref. 5) and PC-MURT simulations (open points). The ARD=176% and there is a vertical offset in effective activation energies of $\sim 30 \text{ kJ/mol}$. However, the PC-MURT correctly predicts that the slope $\partial^2 E_a(T_s) / \partial E_t = -1$, as shown in Table I.

III. RESULTS AND DISCUSSION

The optimal parameters for H₂ dissociation on Cu(111) were obtained by iteratively simulating a variety of state-averaged and eigenstate-resolved experimental data. The PC-MURT parameter set was determined to be $\{E_0 = 79 \text{ kJ/mol}, s=1\}$ based on ARD optimization of the experimental data of Figs. 2 and 3, 5(b) and 7. All PC-MURT calculations reported throughout the paper employ this single set of parameters.

A. Internal state-averaged dissociative sticking and associative desorption

Hydrogen dissociative sticking coefficients derived from experiments^{8,10} employing supersonic molecular beams with heated nozzles are compared with PC-MURT predictions in Fig. 2. The ARD for Fig. 2 is 206% and although the PC-MURT is roughly able to reproduce the order of magnitude of the dissociative sticking, the predictions increasingly diverge from experiment at low normal translational energies. This is predominantly because the slope of the experimental sticking coefficients is steeper than the PC-MURT predicted slope, $\partial S/\partial E_n$. Baer and Mayer⁴⁵ have discussed the dependence of an analogous slope for gas-phase polyatomic molecule dissociation rates on the entropy (i.e., the frequencies and degeneracies) of the transition state. A steep slope indicates a loose transition state and lower vibrational frequencies than in the reactants. Thus, lower transition state frequencies than those of the 6D PES of Nørskov and co-workers might improve the PC-MURT fit to the experimental dissociative sticking coefficients.

The angular flux distributions for hydrogen and deuterium associative desorption^{8,10} are shown in Fig. 3. The PC-MURT predictions are in excellent agreement with experiment giving an ARD of 23%, with theory predicting slightly sharper distributions. Five dimensional quantum scattering calculations²⁶ predict H₂ desorption from Cu(111) at $T_s = 1000 \text{ K}$ should have a $\cos^{25} \vartheta$ angular distribution which seems overly sharp considering that the distribution for H₂ at $T_s = 800 \text{ K}$ is $\cos^{10} \vartheta$ and the distributions generally become broader with increasing surface temperature [cf., $\cos^8 \vartheta$ for H₂ desorption from Cu(100) at $T_s = 1000 \text{ K}$].¹⁸ Somewhat surprisingly, a one-dimensional model developed by van Willigen⁴⁶ calculates the angular distributions well using the equation

$$P(\vartheta) = \frac{E_0 + k_B T \cos^2 \vartheta}{(E_0 + k_B T) \cos \vartheta} \exp\left(-\frac{E_0 \tan^2 \vartheta}{k_B T}\right). \quad (6)$$

The van Willigen model assumes that only normal translational energy E_n aids in overcoming the reaction threshold energy E_0 and that the sticking coefficient is unity for all molecules with $E_n \geq E_0$. The only adjustable parameter within the van Willigen model is the barrier height E_0 which determines the sharpness of the angular distribution. For the angular distributions shown in Fig. 3(a), the van Willigen model⁴⁶ with $E_0 = 24 \text{ kJ/mol}$ reproduced the experimental data with an ARD of just 23%.

TABLE I. Comparison of linear fits to experimental and PC-MURT effective activation energies " $E_a(T_s)$ " as a function of translational energy as displayed in Fig. 5(b).

	H ₂ ($\nu=0, J=1$)/Cu(111)		D ₂ ($\nu=0, J=2$)/Cu(111)	
	Slope	Intercept (kJ/mol)	Slope	Intercept (kJ/mol)
Experiment ^a	-0.92	56	-0.97	62
PC-MURT	-1.00	86	-1.00	94

^aReference 5.

Figure 4 shows mean translational energies as a function of desorption angle for D₂ associative desorption.¹⁸ These data were simulated using the PC-MURT, but were not included in the earlier optimization of the PC-MURT parameters. PC-MURT predictions are for $\langle E_t(\vartheta) \rangle$ to decrease with increasing ϑ , while 5D quantum scattering calculations²⁶ and the van Willigen model yield increasing $\langle E_t(\vartheta) \rangle$ with increasing ϑ . Experimentally, $\langle E_t(\vartheta) \rangle$ stays almost constant as a function of angle through to 35°. The ARD between PC-MURT and experiment is 33%, whereas between the 5D quantum scattering calculations²⁶ and experiment the ARD is 39%. The ARD between the van Willigen model and the experiment is 59%. The mean translational energy as a function of angle in the van Willigen model is

$$\langle E(\vartheta) \rangle = \frac{E_0^2}{(E_0 + k_B T \cos^2 \vartheta) \cos^2 \vartheta} + 2k_B T. \quad (7)$$

While the van Willigen model can reproduce the experimental angular flux distributions with $E_0 = 24 \text{ kJ/mol}$, it predicts that $\langle E_t(\vartheta) \rangle$ goes to infinity as ϑ increases to 90° based on Eq. (7). Although the limiting behavior of the van Willigen model Eq. (7) is unphysical for finite E_0 as $\vartheta \rightarrow 90^\circ$, for $E_0 = 0$ it returns the correct angle-independent result, $\langle E_t(\vartheta) \rangle = 2k_B T_s$. The $\langle E_t(\vartheta) \rangle$ variation predicted by the PC-MURT is the outcome when the activated dissociative sticking obeys normal energy scaling and the pooled energy from many degrees of freedom is available to surmount the activation energy. The limiting PC-MURT value at high angle, $\langle E_t(\vartheta \rightarrow 90^\circ) \rangle = 2k_B T_s$, results from detailed balance because translational energy parallel to the surface does not participate in dissociative sticking and so there is no reactive bias away from the incident translational energy distribution that strikes the surface as $\vartheta \rightarrow 90^\circ$ under thermal equilibrium conditions.

B. Eigenstate-resolved dissociative sticking and associative desorption

Associative desorption experiments by Murphy and Hodgson⁵ revealed the Arrhenius surface temperature dependence of molecular eigenstate-resolved dissociative sticking coefficients and defined effective activation energies for the H₂ and D₂ sticking. PC-MURT predictions of eigenstate-resolved sticking coefficients $S(E_t, E_v, E_r; T_s)$ as a function of inverse surface temperature are compared to relative sticking coefficients measured experimentally in Fig. 5(a). The relative sticking coefficients were scaled by a single factor (i.e., 1/9075.8) to give best agreement with the PC-MURT pre-

dictions of absolute sticking coefficients. Despite the extra freedom necessarily introduced by having to scale the experimental relative sticking data, the ARD=1106% for Fig. 5(a) is high. Figure 5(b) shows the effective activation energies “ $E_a(T_s)$ ” for H₂ and D₂ derived from the data of Fig. 5(a) along with best fit lines as a function of translational energy. There is an offset of ~ 30 kJ/mol in the “ $E_a(T_s)$ ”-intercept values for experiment versus the PC-MURT, but the slopes agree well with $\partial “E_a(T_s)”/\partial E_t \simeq -1$ for both experiment and theory. These values are compared explicitly in Table I.

The PC-MURT can be used to analytically derive $\partial “E_a(T_s)”/\partial E_t = -1$ for a single surface oscillator able to freely exchange energy within the PC and the reactive transition state. We start with the Tolman relationship for the nonequilibrium effective activation energy²⁸

$$“E_a(T_s)” = -k_B \frac{\partial \ln S(T_s)}{\partial (1/T_s)} = \langle E_s \rangle_R - \langle E_s \rangle, \quad (8)$$

$$\langle E_s \rangle_R = \frac{\int_{E_t+E_v+E_r}^{\infty} (E^* - E_t - E_v - E_r) S(E^*) f_s(E^* - E_t - E_v - E_r) dE^*}{\int_{E_t+E_v+E_r}^{\infty} S(E^*) f_s(E^* - E_t - E_v - E_r) dE^*}. \quad (11)$$

The classical surface energy distribution for s surface oscillators can be written as

$$f_s(E_s) = \frac{1}{k_B T_s (s-1)!} \left(\frac{E_s}{k_B T_s} \right)^{s-1} \exp\left(-\frac{E_s}{k_B T_s} \right). \quad (12)$$

Assuming a single surface oscillator participates in the reactive transition state (i.e., $s=1$) and substituting into $\langle E_s \rangle_R$ yields

$$\langle E_s \rangle_R = \frac{\int_{E_t+E_v+E_r}^{\infty} (E^* - E_t - E_v - E_r) S(E^*) (1/k_B T_s) \exp(- (E^* - E_t - E_v - E_r)/k_B T_s) dE^*}{\int_{E_t+E_v+E_r}^{\infty} S(E^*) (1/k_B T_s) \exp(- (E^* - E_t - E_v - E_r)/k_B T_s) dE^*}. \quad (13)$$

All common terms independent of E^* can be brought outside the integrals and canceled, yielding

$$\langle E_s \rangle_R = \frac{\int_{E_t+E_v+E_r}^{\infty} (E^* - E_t - E_v - E_r) S(E^*) \exp(- E^*/k_B T_s) dE^*}{\int_{E_t+E_v+E_r}^{\infty} S(E^*) \exp(- E^*/k_B T_s) dE^*}. \quad (14)$$

Taking the derivative of Eq. (14) with respect to the E_t gives a complicated expression according to the Leibniz integral differentiation formula. However, because the microcanonical sticking $S(E^*)=0$ for $E^* < E_0$ the lower bounds of the integrals can be replaced by E_0 for $E_t < E_0 - E_v - E_r$. Substitution leads to the final result

where $\langle E_s \rangle_R$ is the mean surface energy of the successfully reacting PCs,

$$\langle E_s \rangle_R = \frac{\int_0^{\infty} E_s S(E_s + E_t + E_v + E_r) f_s(E_s) dE_s}{\int_0^{\infty} S(E_s + E_t + E_v + E_r) f_s(E_s) dE_s}, \quad (9)$$

and $\langle E_s \rangle$ is the mean surface energy of all the PCs formed,

$$\langle E_s \rangle = \frac{\int_0^{\infty} E_s f_s(E_s) dE_s}{\int_0^{\infty} f_s(E_s) dE_s}. \quad (10)$$

Since the mean surface energy of all the PCs formed is independent of the molecular translational energy, $\partial \langle E_s \rangle / \partial E_t = 0$, there remains to solve only for $\partial \langle E_s \rangle_R / \partial E_t$. Rewriting $\langle E_s \rangle_R$ in terms of $E^* = E_s + E_t + E_v + E_r$ yields

$$\frac{\partial “E_a(T_s)”}{\partial E_t} = \frac{\partial \langle E_s \rangle_R}{\partial E_t} = \frac{\int_{E_0}^{\infty} (-1) S(E^*) \exp(- E^*/k_B T_s) dE^*}{\int_{E_0}^{\infty} S(E^*) \exp(- E^*/k_B T_s) dE^*} = -1 \quad \text{for } E_t < E_0 - E_v - E_r. \quad (15)$$

Equation (15) also holds true for a single quantum surface oscillator where the density of states is essentially independent of energy [i.e., $\rho(E_s) = \sum_n \delta(E_s - nh\nu_s)$ is a regular picket fence across energy and $h\nu_s$ is small], just like the single classical oscillator. Because the density of states becomes energy dependent for $s > 1$ [e.g., proportional to the preexponential of Eq. (12)] we have not found an analytical route to prove $\partial “E_a(T_s)”/\partial E_t = -1$ for $s > 1$ although numerically this is found to be approximately true for reasonable bounds on s , E_t , E_0 , and T_s .

Figure 6 provides a graphical illustration of how

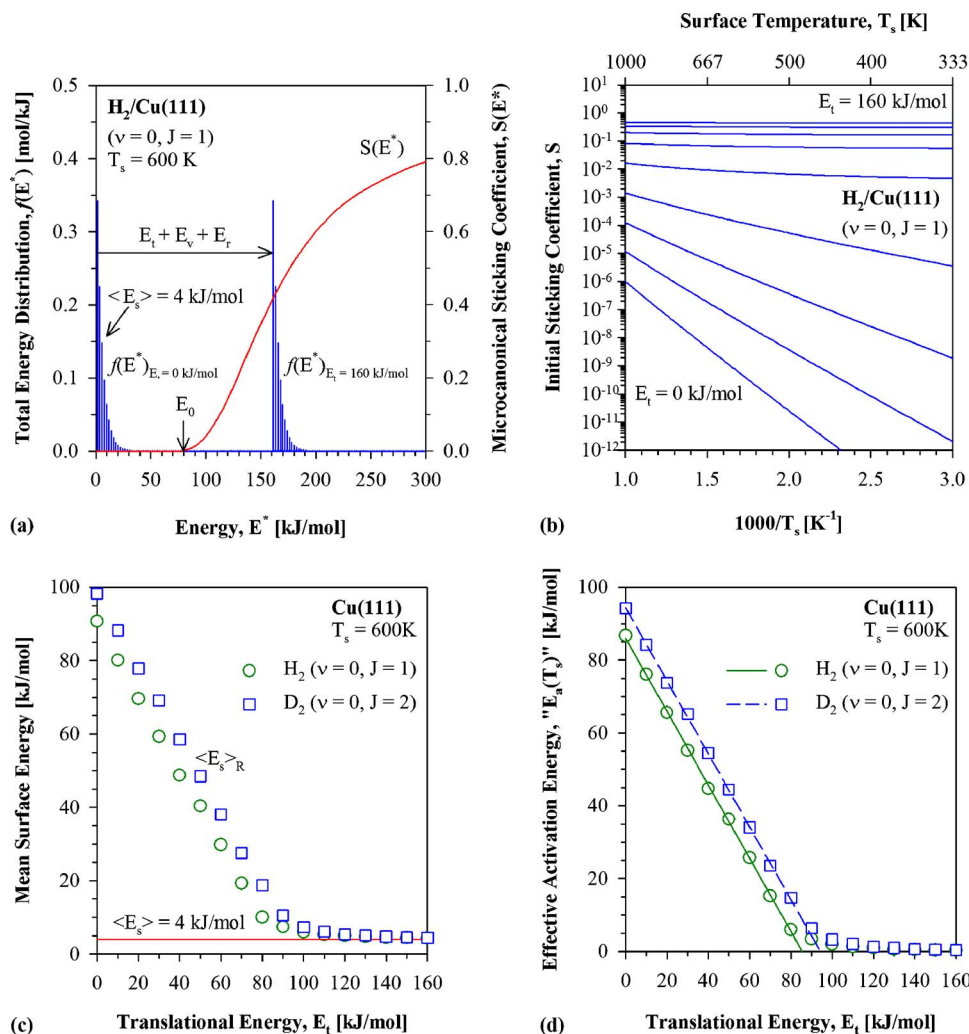


FIG. 6. Surface temperature dependence of molecular eigenstate-resolved dissociative sticking coefficients $S(E_t, E_v, E_r; T_s)$ as E_t is varied. (a) The dissociative sticking is calculated as $S = \int_0^\infty S(E^*) f(E^*) dE^*$, where $E^* = E_t + E_v + E_r + E_s$ and $f(E^*) = f_s(E^* - E_t - E_v - E_r)$ are shown for two E_t values. (b) Arrhenius plots of S as a function of surface temperature over a range of E_t values in increments of 20 kJ/mol. (c) Plotted separately are the mean surface energies for those PCs that successfully react and for all those that are collisionally formed which appear in the Tolman relationship for the nonequilibrium “effective activation energy” “ $E_a(T_s)$ ” = $-k_B \partial \ln S / \partial T_s^{-1} = \langle E_s \rangle_R - \langle E_s \rangle$. (d) Graphical demonstration that $\partial \langle E_a(T_s) \rangle / \partial E_t = \partial \langle E_s \rangle_R / \partial E_t = -1$ for $E_t < E_0 - E_v - E_r$, where “ $E_a(T_s)$ ” values are identical whether they are calculated from the slopes of (b) or directly from (c).

“ $E_a(T_s)$ ” is calculated using Eq. (8), “ $E_a(T_s)$ ” = $-k_B \partial \ln S / \partial T_s^{-1} = \langle E_s \rangle_R - \langle E_s \rangle$. Averaging the microcanonical sticking coefficient $S(E^*)$ over the $f(E^*)$ probability distribution for creating a PC at energy E^* according to Eq. (2) at specific values of E_t , E_v , E_r , and T_s as shown in Fig. 6(a) yields eigenstate-resolved sticking coefficients $S(E_t, E_v, E_r; T_s)$ of the kind displayed in Fig. 6(b). Surface temperature dependent effective activation energies at a specific E_t can be obtained by performing an Arrhenius analysis of the sticking coefficients or from the Tolman relationship defined in Eq. (8). Figures 6(c) and 6(d) graphically demonstrate these two approaches. Equation (11) is used to calculate $\langle E_s \rangle_R$ and Fig. 6(a) shows $f(E^*) = f_s(E^* - E_t - E_v - E_r)$ at two values of E_t : 0 and 160 kJ/mol. A possibly more instructive route for calculating $\langle E_s \rangle_R$ in the context of Fig. 6(a) begins with calculating the mean energy of the reacting PCs,

$$\langle E^* \rangle_R = \int_0^\infty E^* S(E^*) f(E^*) dE^*, \quad (16)$$

and noting that since generally $\langle E^* \rangle_R = \langle E_t \rangle_R + \langle E_v \rangle_R + \langle E_r \rangle_R + \langle E_s \rangle_R$,²⁸ then for these molecular eigenstate-resolved experiments $\langle E_s \rangle_R = \langle E^* \rangle_R - (E_t + E_v + E_r)$. Consider first the case of $f(E^*)$ with $E_t = 0$ kJ/mol. Because E_0 is the threshold energy for reaction and $S(E^*)$ is zero at energies $E^* < E_0$, it is only the high energy tail of the $f(E^*)$ distribution beyond E_0 that contributes to the integral of Eq. (16) that yields $\langle E^* \rangle_R$. The rapidly increasing nature of $S(E^*)$ near threshold tends to skew the mean reactive energy towards higher values and for this example ($E_t = 0$ kJ/mol, $E_v = 0$ kJ/mol, $E_r = 1.4$ kJ/mol), $\langle E^* \rangle_R = 92$ kJ/mol and consequently $\langle E_s \rangle_R = 90.6$ kJ/mol (cf. $E_0 = 79$ kJ/mol). In this instance, almost all of the energy required to surmount the activation barrier derives from the surface. In contrast, when there is molecular

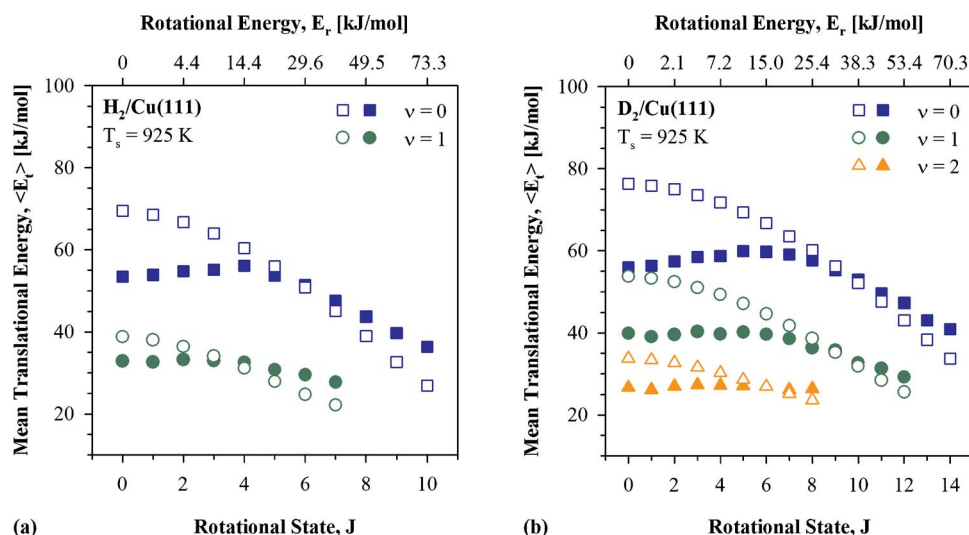


FIG. 7. Experimentally observed mean translational energies (solid points) (Refs. 8 and 10) are plotted as a function of rovibrational state for recombinatively desorbing (a) H_2 and (b) D_2 . PC-MURT simulations (open points) agree well with experiment for $J \geq 5$. The divergence of the experimental results from the theoretical predictions at low J suggests that dynamical steering is important when the angular momentum is low. The ARD for these state-resolved mean energies is 14%.

energy in large excess of the reaction threshold energy, as is the case for Fig. 6(a) $f(E^*)$ distribution with $E_t = 160$ kJ/mol, then the slowly varying nature of $S(E^*)$ at energies well above threshold tends to yield $\langle E^* \rangle_R = \langle E_s \rangle_R + E_t + E_v + E_r$, with $\langle E_s \rangle_R \rightarrow \langle E_s \rangle$. Consequently, at sufficiently high molecular energies “ $E_a(T_s)$ ” = $\langle E_s \rangle_R - \langle E_s \rangle \rightarrow 0$, as illustrated in Figs. 6(c) and 6(d). The flattening of the slope $\partial “E_a(T_s)” / \partial E_t$ away from -1 occurs rapidly after E_t exceeds $\sim E_0$ in Fig. 6(d).

We have rigorously shown above that $\partial “E_a(T_s)” / \partial E_t = -1$ for $E_t < E_0 - E_v - E_r$ and one surface oscillator involved in the physisorbed complex within the PC-MURT model of gas-surface reactivity. By way of comparison, the 5D wave packet calculations of Wang *et al.*¹⁹ involving $\text{D}_2(v=1, J=0)$ reacting with a single surface oscillator of Cu(111) over a reduced dimensionality 4D PES with $E_0(\text{D}_2) \sim 75$ kJ/mol gave $\partial “E_a(T_s)” / \partial E_t = -0.86$ over the E_t range from 29 to 35 kJ/mol with the slope diminishing rapidly towards zero at higher E_t [cf. Fig. 6(d) for $v=0$]. The PC-MURT prediction for the break in the “ $E_a(T_s)$ ” slope away from -1 for $\text{D}_2(v=1, J=0)$ reacting on the PES of Wang *et al.* would be at $E_t \sim E_0 - E_v - E_r \approx 39$ kJ/mol, in reasonable accord with the wave packet calculations.

Mean translational energies for associatively desorbing hydrogen as a function of rovibrational state are plotted in Fig. 7 along with PC-MURT predictions.^{8,10} The ARD between theory and the experiments is 14%. At low rotational quantum number J , the PC-MURT predictions of $\langle E_t(v, J) \rangle$ are substantially higher than experimental values. However, for H_2 with $J \geq 4$ and D_2 with $J \geq 6$ there is good agreement between theory and experiment. The discrepancy at low J suggests that dynamical effects are important at low rotational energy. This discrepancy may be the result of dynamical steering where long range forces from the surface are able to reorient incident molecules into the broadside attack geometry that favors dissociation. As discussed in the Introduction, dynamical steering should fall off in importance with increasing J and E_t of the incident molecules because of the increasing torque required to reorient the molecules during their approach to the surface and the decreasing collision time over which to accomplish the reorientation. Because

dynamical steering involves molecular reorientation accomplished through long range forces before the molecule reaches the transition state, the transition state MURT model cannot account for steering’s effects on the gas-surface reactivity. It may be that low energy collisions in which a molecule is steered into the ideal broadside collision geometry for reaction are less energy randomizing and so reactive channels, rather than the typically more numerous desorptive channels, are relatively more easily accessed [i.e., Eq. (3) statistical limit is not realized]. Such a tendency would raise the sticking coefficients at low translational energies and bring down the $\langle E_t(v, J) \rangle$ values at low J as compared to the statistical limit over the range of E_t and J where steering is significant. At high $J \geq 5$, where steering is unlikely to be important,⁶ theory and experiment agree that $\langle E_t(v, J) \rangle$ falls off with increasing J , consistent with rotational energy participating like normal translational energy in statistically overcoming the activation barrier for dissociation.

A remaining question is whether the modest experimental $\langle E_t(v, J) \rangle$ values within the steering domain at low J are energetically compatible with the reaction threshold energy of $E_0 = 79$ kJ/mol determined by PC-MURT analysis. Taking $\text{H}_2(v=0, J=0)$ associative desorption at 925 K in Fig. 7 as an example, the experimental value of $\langle E_t(v=0, J=0) \rangle$ is 53.5 kJ/mol which must also equal $\langle E_t \rangle_{R, \text{expt}}$ for dissociative sticking from the $\text{H}_2(v=0, J=0)$ state in thermal equilibrium. The PC-MURT prediction for the mean surface energy of PCs formed from successfully reacting $\text{H}_2(v=0, J=0)$ at 925 K is $\langle E_s \rangle_R = 46$ kJ/mol. By detailed balance, the mean energy of the PCs formed from reacting $\text{H}_2(v=0, J=1)$ molecules at 925 K can then be estimated as $\langle E^* \rangle_R = \langle E_t \rangle_{R, \text{expt}} + \langle E_v \rangle_R + \langle E_r \rangle_R + \langle E_s \rangle_R$ which totals 99.5 kJ/mol, more than enough to surmount a reaction threshold energy of 79 kJ/mol. The point is that the surface at a temperature of $T_s = 925$ K is a flexible energy reservoir [e.g., see Fig. 6(c)], typically supplying considerable energy to the reacting PCs, and so the minimum $\langle E_t(v, J) \rangle$ values of Fig. 7 cannot directly define the threshold energy for dissociative sticking on the PES.

The undeniable participation of the surface in the disso-

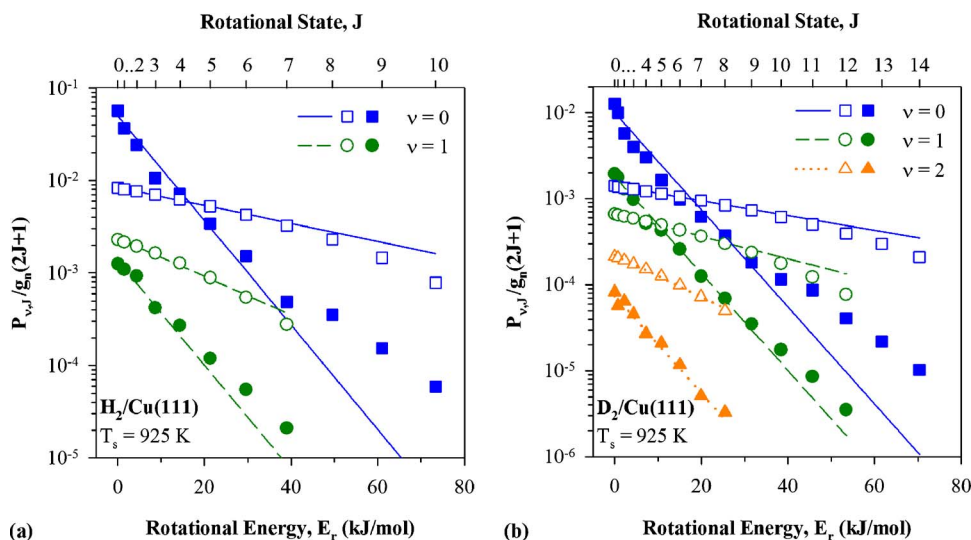


FIG. 8. A comparison of experimental (solid points) and PC-MURT (open points) rotational energy distributions for recombinative desorption of (a) H_2 (Ref. 8) and (b) D_2 (Ref. 10) is presented. Lines through the experiment represent an Arrhenius fit to the low J data assuming that the rotational temperature is equal to the surface temperature (i.e., $T_r = T_s = 925$ K). A similar fit to the PC-MURT predictions yields rotational temperatures of 5571, and 2923 K for H_2 in the $\nu=0$ and 1 states and 6411, 4296, and 2399 K for D_2 in the $\nu=0, 1,$ and 2 states, respectively. The ARD for the rotational energy distributions is 489%.

ciative sticking of hydrogen on Cu(111) is most clearly evident in Murphy and Hodgson's experimental determination of " $E_a(T_s)$ " at low J in Fig. 5(b) where " $E_a(T_s)$ " values can exceed 50 kJ/mol. The ~ 30 kJ/mol offset between experimental and PC-MURT predictions of the " $E_a(T_s)$ " values may be due to dynamical steering effects limited to low J such that agreement between theory and experiment would improve if the experimental measurements were repeated for molecules at high J . Despite the internal inconsistency that the low J sticking diverges from our statistical model's predictions and is presumably influenced by dynamical effects such as steering, let us nonetheless employ the statistical Tolman relation, " $E_a(T_s) = \langle E_s \rangle_R - \langle E_s \rangle$ ", and the assumption that one surface oscillator participates in the reactive PCs to estimate an upper bound for the reaction threshold energy using experimental measures. For the $\text{H}_2(\nu=0, J=1)$ state of Fig. 5(b) with $E_r = 1.4$ kJ/mol at $E_t = 5$ kJ/mol, " $E_a(T_s)$ " is 52 kJ/mol. Assuming a temperature of $T_s = 600$ K, $\langle E_s \rangle = 4$ kJ/mol and so $\langle E_s \rangle_R = "E_a(T_s) + \langle E_s \rangle"$ is 56 kJ/mol. The mean energy of the reacting PCs for $\text{H}_2(\nu=0, J=1; E_t = 5$ kJ/mol) sticking at 600 K is then $\langle E^* \rangle_R = 62.4$ kJ/mol which must exceed E_0 . Based on this somewhat internally inconsistent analysis of the experimental data, E_0 should be less than 62.4 kJ/mol. However, if this were the case, instead of $E_0 = 79$ kJ/mol, it would be impossible to theoretically recover agreement with the experimental falloff of $\langle E_r(\nu, J) \rangle$ at high J using the PC-MURT.

This discrepancy over the upper bound for E_0 makes it worth briefly scrutinizing the robustness of Murphy and Hodgson's⁵ extraction of " $E_a(T_s)$ " values that hinge on consistently normalizing surface temperature dependent, eigenstate-resolved, relative sticking coefficients derived from measurements of eigenstate-resolved translational energy distributions of associatively desorbing molecules at different surface temperatures. By detailed balance, Hodgson employs

$$P(E_t, \vartheta; \nu, J, T_s) \propto f_t(E_t, T_s) S(E_t, \vartheta; \nu, J, T_s) \propto E_t \exp(-E_t/k_B T_s) S(E_t, \vartheta; \nu, J, T_s) \quad (17)$$

to relate the translational energy distribution of associatively

desorbing (ν, J) state-selected (solid molecules) to the flux weighted thermal translational energy distribution times the state-resolved sticking coefficient. Relative $S(E_t, \vartheta; \nu, J, T_s)$ values derived from experiments at different T_s were then normalized to one another under the physically reasonable assumption that the sticking coefficients will go to a common limiting value, independent of the surface temperature, in the limit of sufficiently high E_t (e.g., 100 kJ/mol). Just this kind of T_s -independent sticking behavior is observed at high E_t in Fig. 6(b) according to the PC-MURT. The $P(E_t, \vartheta; \nu, J, T_s)$ translational energy distributions of associatively desorbing D_2 spanned a range of E_t from 0 to 100 kJ/mol which allowed Murphy and Hodgson to directly apply Eq. (17) to normalize the relative sticking coefficient curves to one another using the sticking at high E_t . To avoid using only a limited range of the desorption data at high E_t to normalize the relative sticking curves, Murphy and Hodgson went further and were able to fit the $P(E_t, \vartheta; \nu, J, T_s)$ translational energy distributions over the wide E_t range from 0 to 100 kJ/mol using an empirically derived erf-functional form for the sticking coefficients such that the relative sticking coefficients could be analytically extrapolated to high E_t for consistent normalization. Murphy and Hodgson obtained excellent agreement between the normalization by the erf fitting procedure and by direct inversion of the high E_t experimental data. Although the consistency of the relative sticking curve normalization is clearly important for the eventual extraction of accurate values of " $E_a(T_s)$ " $= -k_B \partial \ln S / \partial T_s^{-1} = \langle E_s \rangle_R - \langle E_s \rangle$, it seems that Hodgson's methods are exemplary. Consequently, for reactive systems that behave statistically [perhaps, not $\text{H}_2/\text{Cu}(111)$], Murphy and Hodgson's new desorption technique for determining " $E_a(T_s)$ " values for molecular eigenstate-resolved sticking coefficients can provide a useful upper bound for the dissociation threshold energy E_0 through calculation of the average energy $\langle E^* \rangle_R$ of the reacting PCs as detailed above.

The rotational distributions for hydrogen and deuterium desorbing from Cu(111) at $T_s = 925$ K are plotted in Boltzmann form in Fig. 8. Experimental values were normalized by asserting $\sum P(E_{\nu, J}) = 1$ over the ν, J range of measured

eigenstates. The PC-MURT $P(E_{\nu,J})$ values sum to 1.000 over the theoretically considered $\nu=0-5$ and $J=0-26$ range of eigenstates and sum to ~ 0.95 over the more limited experimental range of measured eigenstates. The vibrational state-resolved experimental data are well fitted through to $J \sim 7$ by Boltzmann plot lines representing $P_{\nu,J} = g_n(2J+1)\exp(-E_r/k_B T_r)$, where $T_r = T_s$ and g_n is the nuclear spin degeneracy.^{8,10} The PC-MURT predictions do not correlate well with the experimental measurements and the Fig. 8 ARD is 489%. Arrhenius fit lines drawn through the PC-MURT predictions give the following effective rotational temperatures: for H_2 in the $\nu=0$ and 1 vibrational states $T_r=5571$ and 2923 K, respectively, and for D_2 in the $\nu=0, 1,$ and 2 vibrational states $T_r=6411, 4296,$ and 2399 K, respectively (cf. $T_r=T_s=925$ K for experiment at low J). Interestingly, the intersection points between the $\nu=0$ PC-MURT and experimental data are observed at almost the same J states at which the $\langle E_t(\nu,J) \rangle$ values begin to agree in Fig. 7—presumably those J states that mark the end of the domain of dynamical steering. The PC-MURT predicts much higher T_r values than T_s because it assumes that rotational energy is fully participatory in promoting dissociation. Out of a 925 K thermal rotational distribution incident on a surface at thermal equilibrium, rotationally hotter molecules should preferentially dissociatively stick and so by detailed balance a higher T_r should characterize the associatively desorbing molecules. Experimentally, this behavior is clearly not observed at low J where $T_r=T_s$ and one might be tempted to argue that rotational energy is simply a spectator to dissociative chemisorption. The lack of variation of $\langle E_t(\nu,J) \rangle$ with J displayed in Fig. 7 at low J is certainly consistent with this interpretation but why then does experiment follow the PC-MURT $\langle E_t(\nu,J) \rangle$ predictions at higher J ? The answer may be that dynamical steering dominates the sticking at low J and its rolloff in efficacy with J tends to move $\langle E_t(\nu,J) \rangle$ upwards while an increasing efficacy of utilizing rotational energy statistically tends to move $\langle E_t(\nu,J) \rangle$ downwards such that the net experimental result is a relatively flat $\langle E_t(\nu,J) \rangle$ variation with J at low J and hence $T_r=T_s$ in Fig. 8 at low J . Certainly, the experimental associative desorption population in $\nu=0$ at high J in Fig. 8 moves above the $T_r=T_s=925$ K line, consistent with a higher effective rotational temperature and increased utilization of rotational energy in dissociative chemisorption at high J . In summary, although the experimental data of Figs. 7 and 8 support some involvement of rotational energy in promoting the dissociative sticking of hydrogen, at least at high J , the data do not demand complete participation of rotational energy in the way assumed by the PC-MURT.

C. Thermal dissociative sticking

Emboldened by some success at reproducing the results of state-averaged and eigenstate-resolved dissociative sticking experiments, let us now turn to the prediction of thermal dissociative sticking coefficients. Figure 9 displays PC-MURT predictions of $H_2/Cu(111)$ dissociative sticking coefficients for an effusive thermal beam at temperature T_g incident at $\vartheta=0^\circ$ on a surface at temperature T_s , $S(T_g, T_s; 0^\circ)$, and for an ambient gas of temperature T_g inci-

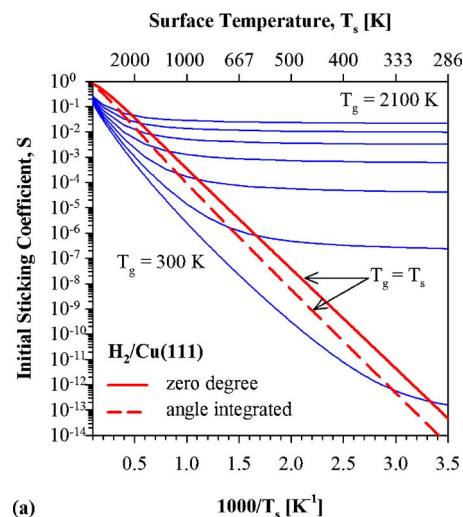


FIG. 9. PC-MURT predictions for the dissociative sticking of H_2 gas as a function of T_g and T_s , assuming that the gas is incident at 0° (solid lines) from an effusive molecular beam source or angle integrated (dashed line) from an ambient random gas onto a Cu(111) surface. The thin lines are for $T_g=300-2100$ K in 300 K increments, while the bold lines are for $T_g=T_s$. The dashed bold line gives the thermal equilibrium sticking.

dent from all angles onto a surface at T_s , $S(T_g, T_s)$. The thermal equilibrium sticking coefficient is $S_T = S(T_g, T_s)$, with $T = T_g = T_s$. The other nonequilibrium sticking coefficients are simply the ones that might be measured using thermally prepared gas and surface at low pressures where T_g and T_s can be independently varied and maintained. A similar family of nonequilibrium $S(T_g, T_s; 0^\circ)$ and $S(T_g=300 \text{ K}, T_s)$ experimental measurements was recently made for CH_4 and C_2H_6 activated dissociative chemisorption on Pt(111).^{39,42} The $H_2/Cu(111)$ thermal sticking coefficient is well described by an Arrhenius expression $S_T = S_0 \exp(-E_a/k_B T)$ where $S_0 = 1.37$ and $E_a = 79.6$ kJ/mol over the temperature range of $300 \text{ K} < T < 2000 \text{ K}$. At sufficiently high T , S_T rolls over to a limiting value of 1. The sticking coefficients of Fig. 9 vary by 14 orders of magnitude and likely underestimate the experimental sticking⁴⁷ because of the relatively high E_0 value used in the PC-MURT calculations and the nonstatistical behavior of hydrogen at the low J states that are most easily thermally accessed (e.g., Fig. 7). The nonequilibrium sticking coefficients generate a variety of opportunities to measure effective activation energies, $\langle E_a(T_s) \rangle = -k_B \partial \ln S / \partial T_s^{-1}$ that are readily interpreted using Eq. (8) Tolman relation $\langle E_a(T_s) \rangle = \langle E_s \rangle_R - \langle E_s \rangle$. For example, $S(T_g, T_s; 0^\circ)$ measurements at relatively high T_g and relatively low T_s in the upper right of Fig. 9 should show $\langle E_a(T_s) \rangle \approx 0$ because the reacting system can use the more flexible high T_g gas heat reservoir to supply virtually all its energy needs to surmount the activation barrier for dissociation. As T_s begins to exceed T_g on the left side of Fig. 9, the system can increasingly draw energy to react from the surface. An important point is that such “effective activation barriers” are very much dependent on the specific experimental conditions of their measurement and are not as easily related to the threshold energy for reaction E_0 as is the thermal activation energy E_a which is generally not more than a few $k_B T$ above E_0 .²⁸

Although the PC-MURT incorporates only a single sur-

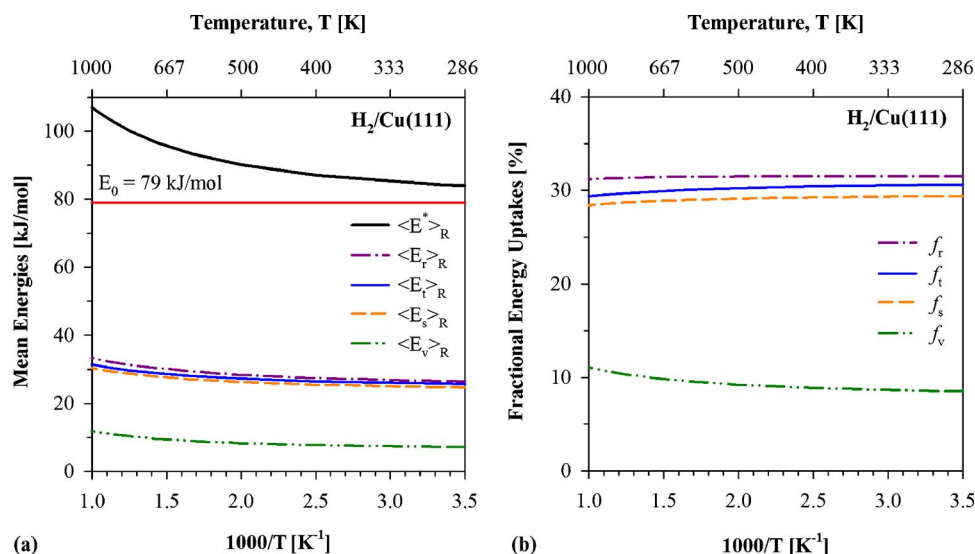


FIG. 10. PC-MURT predictions of (a) the mean energies of the reacting physisorbed complexes that derive from different gas and surface degrees of freedom, and (b) the fractional energy uptakes from the different degrees of freedom [e.g., $f_i = \langle E_i \rangle_R / \langle E \rangle_R$] for thermal sticking. Under thermal equilibrium conditions, about 30% of the energy required to surmount the barrier for dissociative chemisorption derives from the surface phonons.

face oscillator in the reactive transition state, Fig. 10 illustrates why the sticking coefficients of Fig. 9 can exhibit strong variation with T_s . Mean energies for the reactive species and fractional energy uptakes, defined as $f_i = \langle E_i \rangle_R / \langle E^* \rangle_R$ or the mean energy derived from the i th reactant degree of freedom for those PCs that successfully react divided by the mean energy of the reacting PCs, indicate that nearly 30% of the energy necessary to overcome the activation barrier to thermal dissociation derives from the surface phonons. Thus, the surface plays an essential role in the dissociative sticking of hydrogen and should not be discounted in theoretical modeling. Figure 10 shows that for the thermal dissociative chemisorption of H_2 , rotations, normal translation, and surface phonons all have comparable $f_i \sim 30\%$, whereas molecular vibration with $f_v \sim 10\%$ plays a lesser role in overcoming the activation barrier to dissociation according to the PC-MURT.

D. Underpinnings of the PC-MURT model

Figure 11 illustrates the sum of states for reaction and desorption along with the PC density of states for the $\text{H}_2/\text{Cu}(111)$ system using the Beyer-Swinehart-Stein-Rabinovitch⁴⁸ density count method. The $\text{HD}/\text{Cu}(111)$ physisorption well has been experimentally characterized by rotationally mediated selective adsorption where it was found

that physisorbed H_2 is a free rotor with an adsorption energy of $E_{\text{ad}} = 2 \text{ kJ/mol}$ and a vibrational frequency along the direction of the surface normal of $\nu_{\text{ph}} \sim 45 \text{ cm}^{-1}$.⁴⁹ For the purposes of Fig. 11, we have neglected nuclear spin statistics and assumed that the PC of the $\text{H}_2/\text{Cu}(111)$ system has $E_{\text{ad}} = 2 \text{ kJ/mol}$ and $\nu_{\text{ph}} \sim 55 \text{ cm}^{-1}$. The PC density of states exceeds the typical threshold level of 10 states/ cm^{-1} for IVR (Ref. 50) once the energy of the reactive complex E^* exceeds about 50 kJ/mol. Consequently, the PC-MURT's premise that the incident PC energy will become microcanonically randomized, in an ensemble-averaged sense, at energies in excess of the threshold energy for reaction, $E_0 = 79 \text{ kJ/mol}$, may be approximated by some combination of (i) direct collisional mixing as trajectories access the highly anharmonic region of PES in the neighborhood of the transition state⁵¹ and (ii) rapid IVR over the RRKM lifetime for desorption which is $\tau_D \sim 3 \text{ ps}$ at reactive energies.²⁸ Some key observations that tend to support statistical state mixing at reactive energies are that once the threshold energy for dissociation is surpassed, there are more than 1000 open rovibrational channels for desorption [i.e., $W_D^\ddagger(E^* = E_0)$], the PC density of states is greater than 10 states/ cm^{-1} , and the PC will have access to the anharmonic transition state region of the PES. The breadth of the PC energy distribution $f(E^*)$ is always significant, even for the molecular eigenstate-resolved stick-

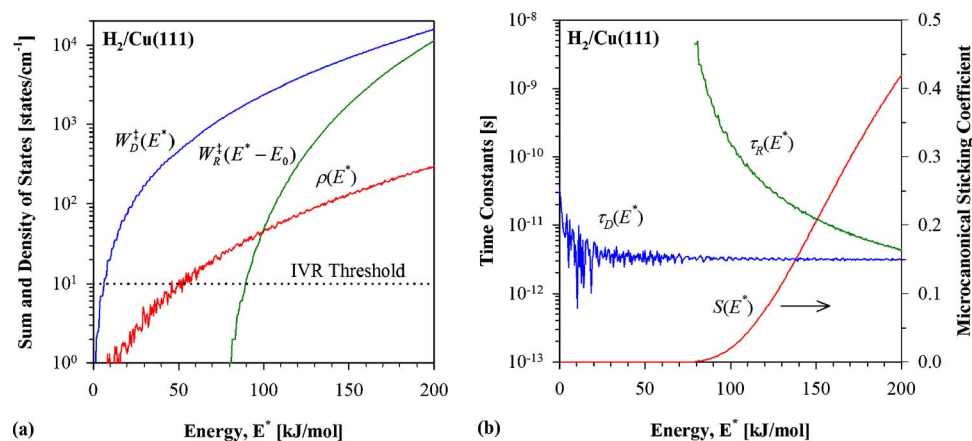


FIG. 11. (a) Desorption and reaction sum of states are shown along with the density of states for the physisorbed complexes. The PC density of states does not reach the intramolecular vibrational energy redistribution (IVR) threshold of 10 states/ cm^{-1} (dotted line) until $E^* \geq 50 \text{ kJ/mol}$. (b) Unimolecular time constants ($k_i(E^*)^{-1}$) for desorption and reaction are shown along with the microcanonical sticking coefficient, $S(E^*) = \tau_D(E^*) / [\tau_D(E^*) + \tau_R(E^*)]$.

ing experiments of Fig. 6(a), because of the breadth of the thermal surface energy distribution. Consequently, calculation of the experimental sticking will usually require considerable energetic averaging of the kind described in Eq. (2). Further ensemble averaging over the molecular vibrational phase, orientation, and impact position across the surface unit cell is also experimentally incurred. It is widely believed that extensive experimental averaging will tend to support a statistical theoretical model even if the statistical limit is only approximated for the microcanonical sticking coefficient of Eq. (3).⁵² This lack of exactness does not detract from the value of a statistical model with few parameters if it captures the essential physics of the reactivity and can accurately predict experimental outcomes. Salin's recent classical trajectory calculations on a 6D GGA-DFT PES with $E_0 = 57$ kJ/mol for H₂ dissociative chemisorption on Cu(110) support a normal over-the-barrier transition state model for hydrogen dissociation on Cu.⁵³ Good agreement with state-averaged experiments was obtained with the high dimensionality trajectory calculations that failed to observe some of the dynamical effects predicted by earlier reduced dimensionality calculations. The gas-surface reactivity was argued to behave more statistically as more of the experimental dimensionality was made theoretically available—an effect commonly observed in studies of gas-phase reactions.⁵⁴ The current two-parameter seven-dimensional (7D) PC-MURT study of hydrogen dissociative chemisorption is believed to treat all the primary molecular and surface degrees of freedom relevant to the reaction because ultrafast desorption of the PCs at reactive energies serves to limit energy dissipation and dynamical involvement of the surrounding surface atoms.

IV. CONCLUSIONS

A simple, two-parameter, full dimensionality, “local hot spot” model of gas-surface reactivity is found to describe much of the state-averaged and eigenstate-resolved dissociative chemisorption and recombinative desorption experiments for hydrogen on Cu(111). The threshold energy for H₂ dissociation is predicted to be $E_0 = 79$ kJ/mol, roughly 50% higher than recent electronic structure theory calculations. Only one surface oscillator participates in the reactive transition state. Nonetheless, the surface phonons are critically important for reactivity, supplying approximately 30% of the energy necessary to surmount the dissociation barrier under thermal equilibrium conditions. The PC-MURT was used to analytically confirm the experimental finding that $\partial \langle E_a(T_s) \rangle / \partial E_t = -1$ for eigenstate-resolved dissociative sticking at translational energies $E_t < E_0 - E_v - E_r$. The discrepancy between associative desorption measurements of hydrogen rotational distributions and $\langle E_t(\nu, J) \rangle$ in low J rotational states with PC-MURT predictions is taken as evidence for the importance of dynamical effects, presumably either dynamical steering or rotational motion acting approximately as a spectator degree of freedom, in the dissociative sticking at low J .

ACKNOWLEDGMENTS

This work was supported by National Science Foundation (NSF), Grant No. 0415540 and by the donors of the American Chemical Society Petroleum Research Fund. One of the authors (H.L.A.) gratefully acknowledges fellowship support under NSF IGERT Grant No. 9972790.

- ¹G. J. Kroes and M. F. Somers, *J. Theor. Comput. Chem.* **4**, 493 (2005).
- ²*Laser Spectroscopy and Photochemistry on Metal Surfaces*, edited by S. F. Bent, H. A. Michelsen, and R. N. Zare (World Scientific, Singapore, 1995), Vol. 2.
- ³H. A. Michelsen, C. T. Rettner, and D. J. Auerbach, in *Surface Reactions*, Springer Series in Surface Sciences, Vol. 34, edited by R. J. Madix (Springer-Verlag, Berlin, 1994), p. 185.
- ⁴S. Nave, D. Lemoine, M. F. Somers, S. M. Kingma, and G. J. Kroes, *J. Chem. Phys.* **122**, 214709 (2005).
- ⁵M. J. Murphy and A. Hodgson, *J. Chem. Phys.* **108**, 4199 (1998).
- ⁶H. Hou, S. J. Gulding, C. T. Rettner, A. M. Wodtke, and D. J. Auerbach, *Science* **277**, 80 (1997).
- ⁷S. J. Gulding, A. M. Wodtke, H. Hou, C. T. Rettner, H. A. Michelsen, and D. J. Auerbach, *J. Chem. Phys.* **105**, 9702 (1996).
- ⁸C. T. Rettner, H. A. Michelsen, and D. J. Auerbach, *J. Chem. Phys.* **102**, 4625 (1995).
- ⁹D. J. Auerbach, C. T. Rettner, and H. A. Michelsen, *Surf. Sci.* **283**, 1 (1993).
- ¹⁰H. A. Michelsen, C. T. Rettner, D. J. Auerbach, and R. N. Zare, *J. Chem. Phys.* **98**, 8294 (1993).
- ¹¹C. T. Rettner, H. A. Michelsen, and D. J. Auerbach, *Chem. Phys.* **175**, 157 (1993).
- ¹²H. A. Michelsen, C. T. Rettner, and D. J. Auerbach, *Phys. Rev. Lett.* **69**, 2678 (1992).
- ¹³C. T. Rettner, D. J. Auerbach, and H. A. Michelsen, *Phys. Rev. Lett.* **68**, 1164 (1992).
- ¹⁴H. A. Michelsen and D. J. Auerbach, *J. Chem. Phys.* **94**, 7502 (1991).
- ¹⁵C. T. Rettner, H. A. Michelsen, D. J. Auerbach, and C. B. Mullins, *J. Chem. Phys.* **94**, 7499 (1991).
- ¹⁶H. F. Berger, M. Leisch, A. Winkler, and K. D. Rendulic, *Chem. Phys. Lett.* **175**, 425 (1990).
- ¹⁷G. Anger, A. Winkler, and K. D. Rendulic, *Surf. Sci.* **220**, 1 (1989).
- ¹⁸G. Comsa and R. David, *Surf. Sci.* **117**, 77 (1982).
- ¹⁹Z. S. Wang, G. R. Darling, and S. Holloway, *J. Chem. Phys.* **120**, 2923 (2004).
- ²⁰S. Sakong and A. Gross, *Surf. Sci.* **525**, 107 (2003).
- ²¹M. F. Somers, S. M. Kingma, E. Pijper, G. J. Kroes, and D. Lemoine, *Chem. Phys. Lett.* **360**, 390 (2002).
- ²²J. Q. Dai and J. C. Light, *J. Chem. Phys.* **108**, 7816 (1998).
- ²³J. Q. Dai and J. C. Light, *J. Chem. Phys.* **107**, 1676 (1997).
- ²⁴P. Kratzer, B. Hammer, and J. K. Nørskov, *Surf. Sci.* **359**, 45 (1996).
- ²⁵B. Hammer, M. Scheffler, K. W. Jacobsen, and J. K. Nørskov, *Phys. Rev. Lett.* **73**, 1400 (1994).
- ²⁶A. Gross, B. Hammer, M. Scheffler, and W. Brenig, *Phys. Rev. Lett.* **73**, 3121 (1994).
- ²⁷Z. S. Wang, G. R. Darling, B. Jackson, and S. Holloway, *J. Phys. Chem. B* **106**, 8422 (2002).
- ²⁸A. Bukoski, D. Blumling, and I. Harrison, *J. Chem. Phys.* **118**, 843 (2003).
- ²⁹H. L. Abbott, A. Bukoski, and I. Harrison, *J. Chem. Phys.* **121**, 3792 (2004).
- ³⁰A. Bukoski, H. L. Abbott, and I. Harrison, *J. Chem. Phys.* **123**, 094707 (2005).
- ³¹M. J. Cardillo, M. Balooch, and R. E. Stickney, *Surf. Sci.* **50**, 263 (1975).
- ³²C. T. Rettner, L. A. Delouise, and D. J. Auerbach, *J. Chem. Phys.* **85**, 1131 (1986).
- ³³A. C. Luntz, *J. Chem. Phys.* **113**, 6901 (2000).
- ³⁴A. C. Luntz and J. Harris, *Surf. Sci.* **258**, 397 (1991).
- ³⁵M. Dohle and P. Saalfrank, *Surf. Sci.* **373**, 95 (1997).
- ³⁶A. D. Kinnersley, G. R. Darling, and S. Holloway, *Surf. Sci.* **377**, 563 (1997).
- ³⁷G. R. Darling and S. Holloway, *J. Chem. Phys.* **101**, 3268 (1994).
- ³⁸H. L. Abbott, A. Bukoski, D. F. Kavulak, and I. Harrison, *J. Chem. Phys.* **119**, 6407 (2003).

- ³⁹K. M. DeWitt, L. Valadez, H. L. Abbott, K. W. Kolasinski, and I. Harrison, *J. Phys. Chem. B* **110**, 6705 (2006).
- ⁴⁰H. L. Abbott and I. Harrison, *J. Phys. Chem. B* **109**, 10371 (2005).
- ⁴¹D. F. Kavulak, H. L. Abbott, and I. Harrison, *J. Phys. Chem. B* **109**, 685 (2005).
- ⁴²K. M. DeWitt, L. Valadez, H. L. Abbott, K. W. Kolasinski, and I. Harrison, *J. Phys. Chem. B* **110**, 6714 (2006).
- ⁴³G. Herzberg, *Molecular Spectra and Molecular Structure I. Spectra of Diatomic Molecules*, 2nd ed. (Van Nostrand Reinhold, New York, 1950).
- ⁴⁴M. Weissbluth, *Atoms and Molecules*, student ed. (Academic, New York, 1978).
- ⁴⁵T. Baer and P. M. Mayer, *J. Am. Soc. Mass Spectrom.* **8**, 103 (1997).
- ⁴⁶W. van Willigen, *Phys. Lett.* **28A**, 80 (1968).
- ⁴⁷C. T. Rettner, H. A. Michelsen, and D. J. Auerbach, *Faraday Discuss.* **96**, 17 (1993).
- ⁴⁸S. E. Stein and B. S. Rabinovitch, *J. Chem. Phys.* **58**, 2438 (1973).
- ⁴⁹U. Harten, J. P. Toennies, and C. Woll, *J. Chem. Phys.* **85**, 2249 (1986).
- ⁵⁰D. J. Nesbitt and R. W. Field, *J. Phys. Chem.* **100**, 12735 (1996).
- ⁵¹V. A. Ukraintsev and I. Harrison, *J. Chem. Phys.* **101**, 1564 (1994).
- ⁵²K. Freed, *Faraday Discuss. Chem. Soc.* **67**, 231 (1979).
- ⁵³A. Salin, *J. Chem. Phys.* **124**, 104704 (2006).
- ⁵⁴R. D. Levine, *Molecular Reaction Dynamics* (Cambridge University Press, Cambridge, UK, 2005).